

Simulation of RI-mode in TEXTOR by the Canonical Profiles Transport Model (CPTM)

Yu.N.Dnestrovskij¹, S.V.Cherkasov¹, S.E.Lysenko¹, K.N.Tarasyan¹
J.Ongena², A.Messiaen² and TEXTOR-94^{2,3} team

¹Russian Research Centre 'Kurchatov Institute', Institute of Nuclear Fusion, Moscow, Russia,

²Laboratoire de Physique des Plasmas-Laboratorium voor Plasmafysica, Ecole Royale Militaire - Koninklijke Militaire School, Brussels, Belgium

³Institut für Plasmaphysik, Forschungszentrum Jülich, D-52425 Jülich, Germany

Abstract. The Canonical Profiles Transport Model (CPTM) is extended to describe both the L- and RI-Modes in the TEXTOR-94 tokamak. The criterion of the L-RI transition is formulated. The sensitivity of the model to a variation of the plasma parameters is investigated. Reasonable quantitative agreement between calculations and experiment is obtained for TEXTOR discharges with a L-RI transition.

1. INTRODUCTION

The Modified Canonical Profile Transport Model (MCPTM) [1-2] describes a plasma transport by the usual set of transport equations, complemented by a differential equation for the canonical profile of the poloidal magnetic field. This equation contains the control parameter λ , which plays the role of a Lagrange parameter for the free energy functional of Kadomtsev [3]. The boundary conditions for this equation include the second derivative of the poloidal magnetic field and define both the parameter λ and the canonical profiles. As a result, the solutions of the transport equations strongly depend on the plasma edge parameters. For large values of λ ("soft" boundary conditions) the L-mode is described by the MCPTM. If λ becomes smaller than a certain threshold value λ_{thr} ("stiff" boundary conditions), a transition to a different confinement mode is obtained due to a change in the form of the canonical profiles and transport coefficients. We identify this mode as the Radiative Improved (RI-Mode) of the TEXTOR-94. In this paper the MCPTM is applied to describe the RI-Mode, obtained on the limiter tokamak TEXTOR-94 by impurity seeding of Ne, Ar or Si [4,5].

2. THE MODIFIED TRANSPORT MODEL

For the simulation of the energy and particle balances in the plasma core we used the set of transport equations for the electron and ion temperatures T_e , T_i , plasma density n and the poloidal magnetic field $\mu=1/q$ [1]. The heat and particle fluxes consist of two terms

$$\Gamma_e = \Gamma_e^{\text{PC}} + \Gamma_e^{\text{an}}, \quad \Gamma_i = \Gamma_i^{\text{PC}} + \Gamma_i^{\text{neo}}, \quad \Gamma_n = \Gamma_n^{\text{PC}} + \Gamma_n^{\text{an}} \quad (1)$$

The convective terms are small in TEXTOR and omitted. The heat fluxes in (1) are given by:

$$\Gamma_k^{\text{PC}} = -n\chi_k^{\text{PC}} \left(\frac{\partial T_k}{\partial r} - \frac{T'_{\text{kc}}}{T_{\text{kc}}} T_k \right), \quad (k=e,i), \quad \Gamma_e^{\text{an}} = -n\chi_e^{\text{an}} \frac{\partial T_e}{\partial r}. \quad (2)$$

The particle fluxes have the same structure. The term Γ_i^{neo} is the neoclassical ion heat flux. The functions $T_{\text{ec}}(r, t) = T_{\text{ic}}(r, t) = T_c(r, t)$, $n_c(r, t)$ are the canonical profiles for the electron and ion temperatures and plasma density. The canonical profile for the poloidal magnetic field $\mu_c = \mu_c(r, t)$ has to satisfy an Euler equation [2, 3]

$$\frac{d}{dr} \left(\mu_c^2 + \lambda \mu_{ca} a^2 \frac{d\mu_c}{d(r^2)} \right) = 0, \quad (3)$$

where $\mu_{ca} = \mu_{ca}(t) = \mu_c(r=a, t)$. For the L-mode we use the canonical profiles of Kadomtsev

$$\mu_c^K = \mu_0 / (1 + r^2/a_j^2), \quad a_j^2 = a^2 (\mu_a / (\mu_0 - \mu_a)), \quad \mu_0 = \mu_c^K(0) \sim 1. \quad (4)$$

This is the solution of the Eq. (3), which tends to zero as r goes to infinity.

For the RI-Mode we propose the following boundary conditions for Eq. (3) [2].

$$\mu_c(a, t) = \mu(a, t), \quad \mu_c'(a, t) = \mu'(a, t), \quad \mu_c''(a, t) = \mu''(a, t) \quad (5)$$

where $\mu(r, t)$ is the solution of the diffusion equation for the poloidal magnetic field.

Using (3) and (5), we obtain the following expression for λ :

$$\lambda = \frac{4}{1 - a\mu_a''/\mu_a'} \approx \left(1 + \frac{a\sigma_a'}{4\sigma_a} \left(\frac{j_a}{\bar{j} - j_a} \right) \right)^{-1}, \quad (6)$$

where $\sigma_a = \sigma(a, t)$ and $j_a = j(a, t)$ are the plasma conductivity and the current density at the edge, $\sigma' = \partial\sigma/\partial r$, $\bar{j} = I/\pi a^2$, I is the plasma current. For the L-mode we have [1]

$$T_c(r)/T_c(0) = n_c(r)/n_c(0) = [\mu_c(r)/\mu_c(0)]. \quad (7)$$

We assume in this work that the relations (7) are satisfied for the RI-Mode also.

For the canonical profiles of Kadomtsev $\lambda = \lambda^K = 1/(1 - \mu_a/\mu_0) \sim 1 + \mu_a/\mu_0$.

We now make the proposition that the value of $\lambda = \lambda^K$ distinguishes between the L- and RI-Modes in the model. In practice, this means that

- the L-mode is realized, if $\lambda > \lambda_{thr} = 1 + \mu_a/\mu_0$, (8.1)

- the RI-mode is realized, if $\lambda < \lambda_{thr} = 1 + \mu_a/\mu_0$. (8.2)

The physical meaning of the model is as follows. If the “real” boundary conditions are “soft” (the boundary temperature is not very low, the edge radiation is not very high, the Z_{eff} profile is flat enough), the plasma core does not “feel” these conditions and boundary conditions for the canonical profiles can be formulated at infinity (Kadomtsev case). In the opposite case of “stiff” boundary conditions (low $T_{e,i}(a)$, large edge radiation, jump of Z_{eff} at the plasma edge) the behavior of the core plasma is strongly linked to the conditions at the plasma edge (5). For the L-mode the transport coefficients have the form [1,2]:

$$D^{an} = D_0 \chi_e^{an}, \quad D^{PC} = C_0 \chi_e^{PC}, \quad (9)$$

$$n\chi_k^{PC} \text{ (L-mode)} = \alpha_k^{PC} \lambda(a/R)^{0.75} q(a/2) q(a) (T_k(a/4))^{0.5} \bar{n} / B = \text{const}(r), \quad (10)$$

$$\chi_e^{an} = \text{const}(r) = \alpha_e \frac{(T_e(a/2))^{1/2}}{n(a/2)R} f_e^{an}(q, a/R), \quad f_e^{an} = 9.4 (4/q_a) (a/R)^{2.5}, \quad (11)$$

$$\alpha_e = 2 \div 4, \quad \alpha_e^{PC} = 3.5, \quad \alpha_i^{PC} = 5, \quad C_0 = 0.8, \quad D_0 = 0.5,$$

where T in keV, B in Teslas, a and R in m, n in 10^{19}m^{-3} , χ_k in m^2/s .

In the RI-mode the energy confinement time rises linearly with the density [4]. So, using Connor’s constraints, we choose the following scaling for the heat diffusivities:

$$n\chi_k^{PC} \text{ (RI-mode)} = 10 \cdot \alpha_k^{PC} (a/R)^{0.75} q(a/2) (T_k(a/4))^{0.5} / R \quad (k=e,i) \quad (12)$$

3. SENSITIVITY STUDIES OF THE MODEL FOR L-MODE AND RI-MODE

For a first test of the model we choose the parameters of the shot #74166

$$R=1.75 \text{ m}, a=0.46 \text{ m}, B=2.25 \text{ T}, I=0.41 \text{ MA}, q_a = 3.8, \mu_a = 1/q_a = 0.265. \quad (13)$$

We suppose that the radiated power profile Q_{rad} is peaked at the plasma periphery after the

impurity seeding and introduce the notations: $P_{\text{rad}}^{\text{edge}} = \int_{0.8a}^a Q_{\text{rad}}(r) r dr$, $\gamma_R = P_{\text{rad}}^{\text{edge}} / P_{\text{tot}}$.

The dependence of the parameter λ on the density \bar{n} for the L- and RI-Modes are shown in Fig.1 a,b for different radiated power fractions γ_R and $Z_{\text{eff}}=\text{const}(r)=2$. Figure 1a relates to the OH (Ohmic heating) regime, Fig.1b relates to discharges with auxiliary heating with total heating power $P_{\text{tot}}=2.5$ MW. The range of the threshold parameter $\lambda_{\text{thr}}=1+\mu_a/\mu_0=1.22-1.17$ ($\mu_0 = 1.2-1.5$) is shown by the dashed lines. The uncertainty in λ_{thr} is caused by the uncertainty in the parameter μ_0 . Figure 2 shows that λ decreases with increasing radiation and plasma density (at $P_{\text{tot}}=2.5$ MW, $Z_{\text{eff}}=2$). The curves separating the L- and RI-Mode in the plane (P_{tot}, γ_R) for different plasma densities are shown in Fig. 3.

4. SCALINGS FOR THE ENERGY CONFINEMENT TIME

It is well known from the experiment that two modes can exist in the OH regime: these are the SOC (saturated) mode and IOC (improved) mode. According to our model, the SOC and IOC modes are equivalent to the L- and RI-Modes. We consider the behavior of these modes separately for the parameters (13) and $Z_{\text{eff}} = 2$. The energy confinement time τ_E as a function of the line-averaged density \bar{n} is shown in Fig. 4. The location of the experimental points [4,5] in this and next figures are indicated by the dashed curves. It is seen that τ_E is saturated for the L (SOC) mode and linearly depends on the density for the RI (IOC) mode.

In the regime with additional heating the L-RI transition occurs “naturally” through the increase of the edge radiation. In Figures 5 and 6 we compare the predicted steady-state values of τ_E and stored energy W with the experimental values [4,5] as a functions of the plasma density. The results of the calculations for the L-mode ($\bar{n} < 5$) and RI-mode ($\bar{n} > 4$), for two values of the total heating power ($P_{\text{tot}}=2$ and 2.5 MW), are shown by the solid lines. Also Fig. 6 shows W for the OH regime. In all cases a reasonable agreement is reached between the experimental values and the predictions of the model.

5. CONCLUSIONS

The Modified Canonical Profiles Transport Model (MCPTM) is applied to describe the RI-Mode in TEXTOR. The transition from L to RI-Mode happens naturally in the framework of the model developed. For the Ohmic heating regime the MCPTM allows us to describe both the SOC and IOC confinement regime by the proposition that SOC regime corresponds to the L-Mode and IOC regime to the RI-Mode.

The authors thank Dr. A.Yu. Dnestrovskij for useful discussions. This work was supported by the WTZ Agreement (97-98, p. 5.64) and by the UKAEA Consulting Agreement GQ13158.

REFERENCES

- [1] DNESTROVSKIJ, Yu.N., et al., Plasma Phys. Reports **23** (1997) 566.
- [2] DNESTROVSKIJ, Yu.N., et al., Nucl. Fusion **38** (1998) 373.
- [3] KADOMTSEV, B.B. Sov. J. Plasma Phys. **13** (1987) 11.
- [4] MESSIAEN, A.M., ONGENA, J., et al., Phys. Rev. Letters, **77** (1996) 2487.
- [5] MESSIAEN, A.M., ONGENA, J., et al., Phys. Plasmas **4**(1997) 1690.

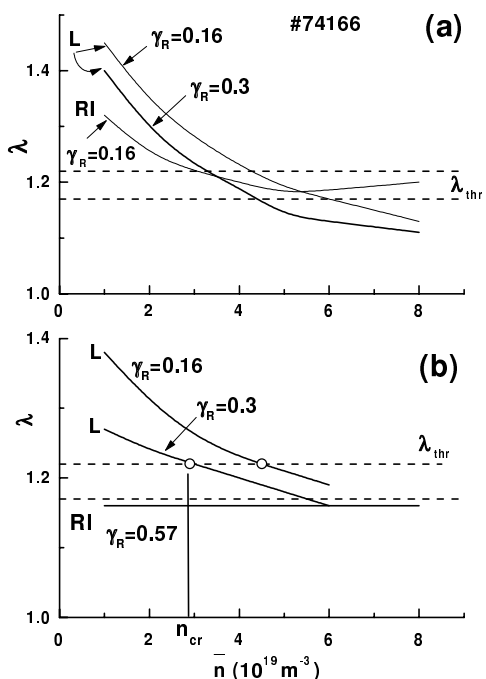


Fig.1

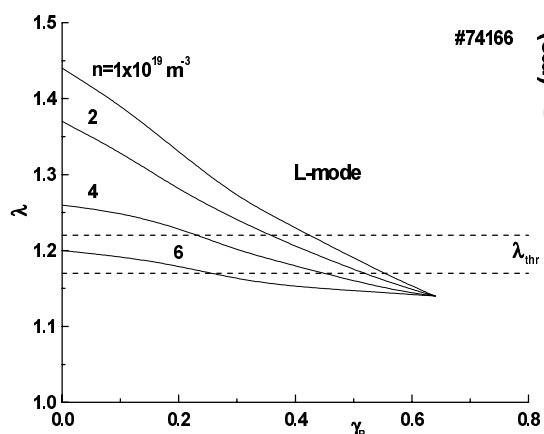


Fig.2

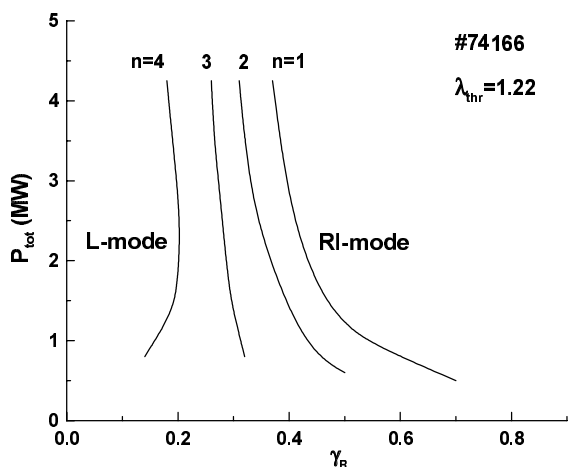


Fig.3

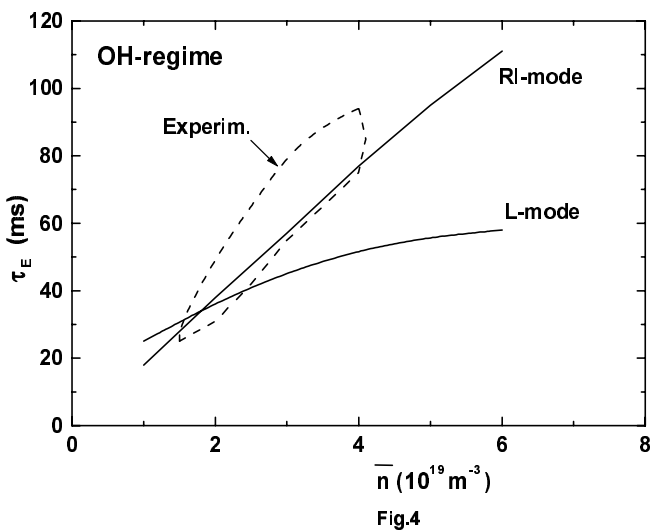


Fig.4

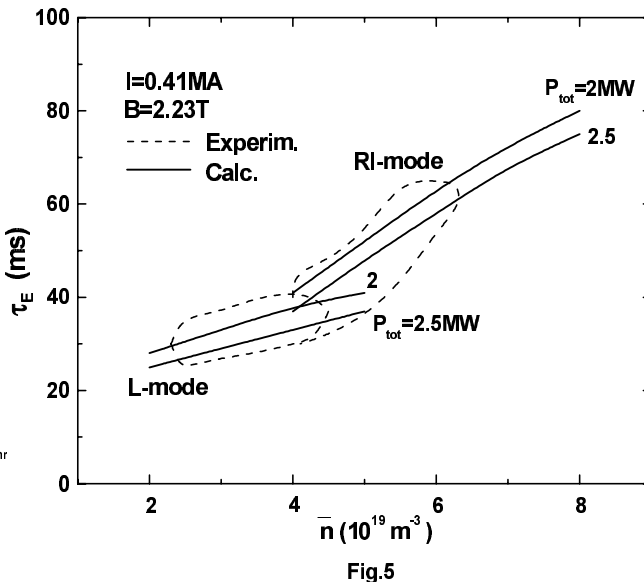


Fig.5

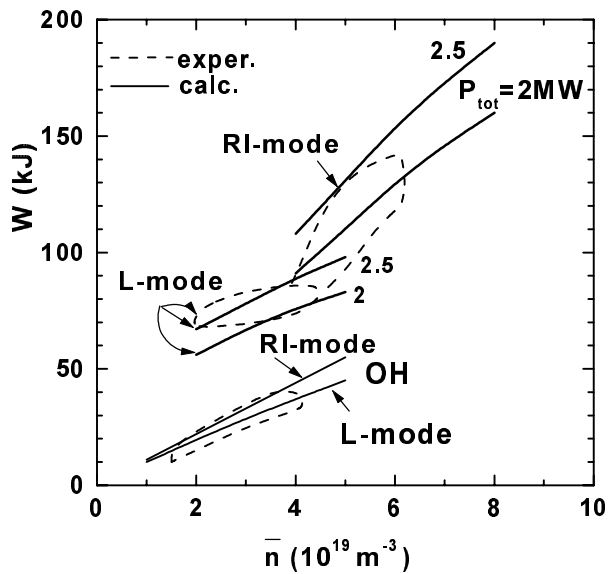


Fig.6